Construction and Building Materials 80 (2015) 105–115

Contents lists available at ScienceDirect

Construction and Building Materials

journal homepage: www.elsevier.com/locate/conbuildmat

Reaction kinetics, gel character and strength of ambient temperature cured alkali activated slag–fly ash blends

X. Gao, Q.L. Yu *, H.J.H. Brouwers

Department of the Built Environment, Eindhoven University of Technology, P.O. Box 513, 5600 MB Eindhoven, The Netherlands

HIGHLIGHTS

- Slag/fly ash ratio and activator modulus show synergetic effects on reaction.
- Activator modulus has a more significant influence on early age reaction.
- Gel structures remain stable regardless of activator modulus and slag/fly ash ratio.
- Slag content shows a dominating effect on compressive strength.

ARTICLE INFO

Article history:
Received 24 September 2014
Received in revised form 10 January 2015
Accepted 13 January 2015

Keywords:
Alkali activation
Ambient temperature
Slag–fly ash blends
Reaction kinetics
FTIR
TG/DSC
Compressive strength

ABSTRACT

Room temperature cured alkali activated slag/fly ash blends have shown their advantages in field applications. Given that alkali activated materials are extraordinarily sensitive to the composition of the starting materials, identifying their influences is essential for their application. This paper focuses on the effects of two compositional factors: activator modulus (SiO_2/Na_2O from 1.0 to 1.8) and slag/fly ash mass ratios (between 90/10 and 50/50) on reaction kinetics, gel characters and compressive strength. The results show that when lowering the activator modulus, the early age reaction is significantly accelerated with a higher reaction intensity, and increasing the slag content also leads to an increased reaction rate, especially at low activator modulus. Regardless of the two influential factors, the main reaction products are chain structured C-A-S-H gels with similar water contents and thermal properties, and no typical N-A-S-H type gels are formed in the system. Slight differences in terminal Si—O bonds and crystallization temperature are caused by the activator modulus and slag/fly ash mass ratios, respectively. The compressive strength results show that the optimum activator modulus changes with the slag/fly ash mass ratio, and higher slag/fly ash mass ratios prefer higher activator moduli in general, while either too high or too low activator modulus has detrimental effect on strength. Understanding the reaction, gel structure and strength changes are fundamental for determining key manufacturing parameters and tailoring the properties.

1. Introduction

Alkali activated material has attracted great attention in recent years due to its excellent performances such as mechanical properties [1–3], durability [4–7], thermal stability [8,9] and low environmental impacts [10]. It is usually produced by mixing alkaline activator solutions with solid raw materials. Alkali activated systems can be classified into two types: calcium and silica enriched (Ca + Si) system and aluminosilicates dominated (Si + Al) system [11]. The represented precursor of calcium enriched system is ground granulated blast furnace slag (GGBS), and the reaction product is a C-S-H (I) type gel with a lower Ca/Si ratio and a high Al incorporation [12]. While the typical starting materials of Si + Al system are class F fly ash or metakaolin, having N-A-S-H type gels with three-dimensional network as the major final product [13].

Recently, there is a growing interest of mixing two different alkali activation systems together to form a blended Na_2O–CaO–Al_2O_3–SiO_2 system as several improved properties can result, including modified setting times [14], improved workability [15], reduced shrinkage [16], enhanced mechanical properties and durability [17]. Later studies were focused on understanding the gel compatibility and phase composition in the blended system: generally, both coexistence and interactions take place between C-A-S-H and N-A-S-H type gels [11,18]. Two typical gels can form

* Corresponding author. Tel.: +31 (0)40 247 2371; fax: +31 (0)40 243 8595.
E-mail address: q.yu@bwk.tue.nl (Q.L. Yu).

http://dx.doi.org/10.1016/j.conbuildmat.2015.01.065
0950-0618/

simultaneously within one system [19]; the presence of calcium leads to the formation of C-A-S-H type gels and destroys the N-A-S-H gel structure to some degree by partially replacing sodium with calcium to form (N,C)-A-S-H gels [20–22], while the increased availability of aluminates strongly influences the C-S-H composition and structure [23]. In addition, a higher degree of cross-linking within the reaction products is achieved [24]. Those investigations in the microstructural understanding provide solid theoretical support for further researches on blended alkali activated system.

It has been known that in alkali activated Ca + Si or Si + Al system, the silicate from activator participates in the formation of hydrated C-A-S-H or N-A-S-H gels together with solid silicate sources, and there exists an optimal silicate content in terms of mechanical properties, either insufficient or excessive silicate supply may restrict the formation of an ideal gel structure and lead to a matrix with relatively low strength [25]. Also, the relations between the silicate content and mechanical properties were well established in the individual system [2,25,26]. However, in the case of alkali activated blended systems such as slag/fly ash, the raw material composition plays a more complex role: the silicate from the activator may involve in the formation of all type of typical hydrated gels such as C-A-S-H, N-A-S-H and (N,C)-A-S-H; the silicate from different raw materials may exhibit different de-polymerization rates and availability under different conditions such as curing temperature and alkaline concentration. Thus despite a consensus about the binding mechanisms has been reached in the previous studies, different conclusions were drawn in determining the optimal parameters in strength: some studies showed a decrease in compressive strength with the increase of fly ash content, such as Weiguo et al. [27]; Kumar et al. [28] and Garcia et al. [18]. While other studies indicated that there is an optimum ratio between slag and fly ash, for instance Chi and Huang reported the critical fly ash content is 50% [29], a 20% fly ash content by Yang et al. and a 65% fly ash content by Zhang et al. [30–31]. Differences in critical raw materials' relative content and activator parameters were also reported [15,32–35]. Different used activators and curing conditions make it difficult to make valid comparison between those studies. Therefore, in order to tailor the properties of alkali activated slag/fly ash blends for desired applications, it is necessary to carry out a systematic study considering the effects of raw materials, activators and curing conditions simultaneously.

On the other hand, alkali activated materials manufactured under ambient temperature exhibit several superiorities in field application, but there exists limited studies about the combined influence of activator and raw materials on the comprehensive properties of room temperature cured slag/fly ash mixtures. In this paper, a preliminary study for tailoring the properties of alkali activated slag/fly ash blends was carried out, and the influences of activator modulus and slag/fly ash ratios on reaction, gel characters and strength were addressed. Slag dominated mixes (at least 50% by mass) were chosen due to the superior mechanical properties under room temperature, different slag/fly ash ratios were used to give different starting $CaO–Al_2O_3–SiO_2$ compositions; different activator moduli were used to provide various levels of extra silica, and the constant total Na_2O content was applied to exclude its influence on total extra silicate content. The reaction kinetics and gel characters were investigated by isothermal calorimetry, Fourier transform infrared spectroscopy (FTIR) and thermogravimetry/differential scanning calorimetry (TG/DSC) analysis.

2. Experimental study

2.1. Materials

The solid materials used in this study were ground granulated blast furnace slag (GGBS, supplied by ENCI B.V., the Netherlands) and Class F fly ash according to ASTM C 618 (supplied by Vliegasunie B.V., the Netherlands) [36]. The median particle size (d50) is 27.16 μm for slag and 22.06 μm for fly ash. The chemical compositions of slag and fly ash were analyzed by X-ray fluorescence, and the result is shown in Table 1. The alkali activator used was a mixture of sodium hydroxide pellets (analytical level) and sodium silicate solution that is composed of 27.69% SiO_2, 8.39% Na_2O and 63.9% H_2O by mass. The desired activator moduli (Ms, SiO_2/Na_2O molar ratio) were achieved by adding different amounts of sodium hydroxide pellets into sodium silicate solution, the solution after mixing was cooled down to ambient temperature prior to use. Distilled water was added in order to reach the desired water/binder ratio.

2.2. Sample preparation

In the mix design stage, the equivalent sodium oxide (Na_2O) content was kept at 5.6% by mass of the binder in all samples, five levels of activator moduli (Ms from 1.8 to 1.0) were used (assigned as A to E) to provide different extra silicate contents from activator to the solid material. The fly ash/slag ratios of 90/10, 80/20, 70/30, 60/40 and 50/50 by mass were used (represented as 1 to 5). The water/binder ratio was kept constant as 0.35; the water consisted of the water added from distilled water and the water contained in the original sodium silicate solution. The chosen Na_2O content and water/binder ratio were preliminarily determined that would provide sufficient alkalinity without efflorescence and satisfying flow ability, respectively. The detailed information of mix proportions is listed in Table 2. Paste samples were prepared using a laboratory mixer, the solid materials were added into the mixer followed by activating solution, then the mixtures were mixed at a slow speed for 30 s, and stopped for 30 s before another 120 s at a medium speed. The fresh paste was poured into plastic molds of $40 \times 40 \times 160$ mm^3 and vibrated for 1 min, then covered with a plastic film on the top surface for 24 h; finally all specimens were demolded and cured at 20 °C and relative humidity of 95% until the testing age.

2.3. Testing methods

The compressive strength tests were carried out according to BS EN 196-1 [37]. $40 \times 40 \times 40$ mm^3 cubes were prepared and tested at the ages of 7 and 28 days respectively, and the strength value for each mix was obtained from the average of six specimens. The isothermal calorimetry analysis was conducted under a constant temperature of 20 °C for 72 h. Solid raw materials were firstly mixed with the activating solution for about 1 min, then the mixed paste was transferred into the ampoule and loaded into the calorimeter. Fourier Transform infrared spectroscopy (FTIR) measurement was performed in a Varian 3100 instrument with the wavenumbers ranging from 4000 to 600 cm^{-1} at a resolution of 1 cm^{-1}, and each sample was scanned for 50 times. Thermogravimetry and differential scanning calorimetry (TG/DSC) analysis was conducted in a STA 449-F1 instrument, grinded powder samples were firstly heated to 105 °C and held for 2 h, then up to 1000 °C, both at 5 °C/min with nitrogen as the carrier gas. Both FTIR and TG/DSC analysis to the samples were carried out at the age of 28 days.

Table 1
Major chemical compositions of the raw materials.

Oxides (%)	Fly ash	GGBS
SiO_2	54.6	35.5
Al_2O_3	24.36	13.6
CaO	4.44	38.6
MgO	1.43	10.2
Fe_2O_3	7.2	0.48
Na_2O	0.73	0.35
K_2O	1.75	0.48
SO_3	0.46	1.27
LOI	2.80	1.65

Table 2
Mix proportions of AA-slag/fly ash pastes.

	Slag/fly ash	Na (%)	Activator modulus					W/B
			A	B	C	D	E	
1	90/10	5.6	1.8	1.6	1.4	1.2	1.0	0.35
2	80/20	5.6	1.8	1.6	1.4	1.2	1.0	
3	70/30	5.6	1.8	1.6	1.4	1.2	1.0	
4	60/40	5.6	1.8	1.6	1.4	1.2	1.0	
5	50/50	5.6	1.8	1.6	1.4	1.2	1.0	

3. Results and discussion

3.1. Reaction kinetics

The isothermal calorimetric analysis was conducted on the samples with the activator moduli of 1.8, 1.4, 1.0 (assigned as A, C, E) and slag/fly ash mass ratios of 90/10, 70/30, 50/50 (represented by 1, 3 and 5). Fig. 1 illustrates the heat evolution curves within the first 72 h. The entire reaction processes can be divided into four stages, namely initial dissolution, induction, acceleration/deceleration and stable period. Two calorimetric peaks are shown in all samples: an initial peak with significant high heat flow during the first few minutes and an acceleration peak with relatively low intensity at around 6 to 24 h. The occurrence of two typical peaks is in agreement with the heat evolution curves of silicate activated slag or its blends observed in previous studies [38–40]. The first peak of heat flow corresponds to the initial wetting, dissolution of raw materials (primarily the breakdown of Me—O and T—O bonds of slag) within the first few minutes after mixing [41], also partly due to the formation of the initial reaction products from the dissolved units such as Si, Ca and Na in the solution [42]. The presence of the early peak is generally regarded as a physical rather than a chemical progress. The acceleration peak (i.e., the second peak) observed at over 6 h is assigned to the massive formation of reaction products [43].

Fig. 1(a) shows the heat flow of samples with an activator modulus of 1.8 and slag/fly ash mass ratios of 90/10, 70/30 and 50/50 (A1, A3 and A5). It can be seen that the initial dissolution peak appears at around 3–4 min, samples with a higher slag content resulted in a higher dissolution heat flow, which demonstrates that slag is easier to dissolve than fly ash in alkali solutions under ambient temperature. After the initial dissolution stage, all mixes exhibit an induction period that lasts about 4 to 10 h before the second heat evolution peak. The dissolution of solid precursors in alkali solution leads to the dissolution of the glassy structure of slag and the release of Ca, Si and Al units. The newly formed reaction products from those released units may grow rapidly and form a layer on the surface of unreacted slag particles [44], which limit the amount of available alkalis for slag dissolution and reduce the heat evolution. Because of the continuous alkali supply of sodium silicate and the penetration of alkalis through the newly formed layer [40,45], further reaction continues and the second peak of heat flow appears. Samples with a higher fly ash content present a considerably longer induction time, this is probably due to the low reactivity of fly ash, and it may mainly work as a nuclear site for the reaction products and has a negative contribution to the further reactions between alkalis and slag particles. The second heat evolution peak appears at around 13 h for the sample with a slag/fly ash mass ratio of 90/10, this peak shifts to longer times with lower intensities and broader peak shapes as the fly

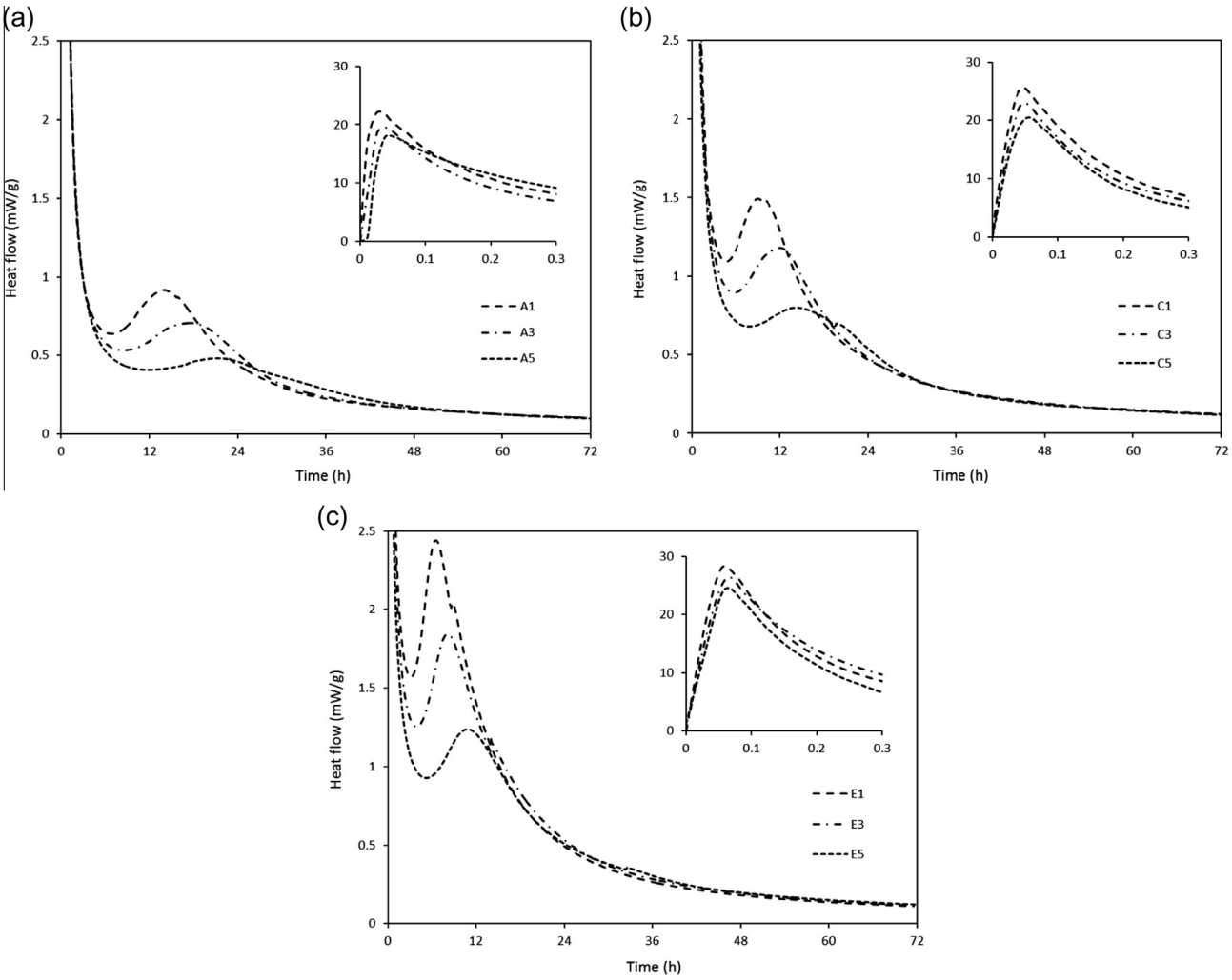

Fig. 1. Heat evolution of AA-slag/fly ash blends [with activator moduli of 1.8 (a), 1.4 (b) and 1.0 (c)].

ash content increases. For instance, when increasing the fly ash content from 10% to 50%, the acceleration peak is delayed for 9 h and the peak height decreases by nearly 47%. Such significant changes are mainly due to the reduced total slag content that resulted in a smaller overall heat evolution, also partly because of the relatively low reactivity and a more moderate reaction process of fly ash under ambient temperature.

Fig. 1(b and c) exhibit the heat evolutions of slag/fly ash blends activated with the activator moduli of 1.4 and 1.0, respectively. It can be seen that as the activator modulus decreases, no significant change takes place in the time of dissolution peak, which proves again that the dissolution stage is more likely a physical process. However, the intensity of the initial peak is considerably increased for all slag/fly ash ratios, indicating a more intensive dissolution and reaction process at the beginning stage. Higher peak flows are also observed in the acceleration stage for all slag/fly ash mixtures, which may indicate a higher reaction degree due to the larger covered area under the peak. The increased reaction caused by the reduction of activator modulus is also found in previous investigations [40,46–47]. It was suggested that a decrease in activator modulus leads to a higher alkali concentration, thus enhancing the dissolution rate and reaction degree of slag [12], a higher alkalinity also increases the solubility of silica and alumina in solution that could benefit the formation of reaction products [48,49]. In addition, a ^{29}Si NMR investigation from a previous study also suggested that a decreased activator modulus resulted in a higher amount of silicate units with low polymerization degree [50]. For a constant slag/fly ash mass ratio, the duration of the induction time significantly decreases when lowering the activator modulus, as can be seen from those figures that the curves representing induction period become narrower and sharper. Furthermore, the commence time of the acceleration peak is decreased, such as from 13 to 6 h in slag/fly ash mass ratio of 90/10 mixes and from 22 to 10 h in slag/fly ash mass ratio of 50/50 mixes. Those reduced induction times and advanced second peak times also demonstrate an acceleration in reaction that is caused by the decreased activator modulus. It should be noted that the reaction process of samples with a high fly ash content was accelerated even more significantly, which indicates that the dissolution of Si—O and Al—O bonds in fly ash also increases to some extent in high alkalinities and contributes to the reaction processes [51].

Fig. 2 shows the cumulative heat evolution of all mixes. The sharp increase at the beginning corresponds to the initial wetting and dissolution of slag in alkali solutions; the relatively moderate increase after the initial stage is associated with the induction period; the acceleration/deceleration period is represented by the dra-

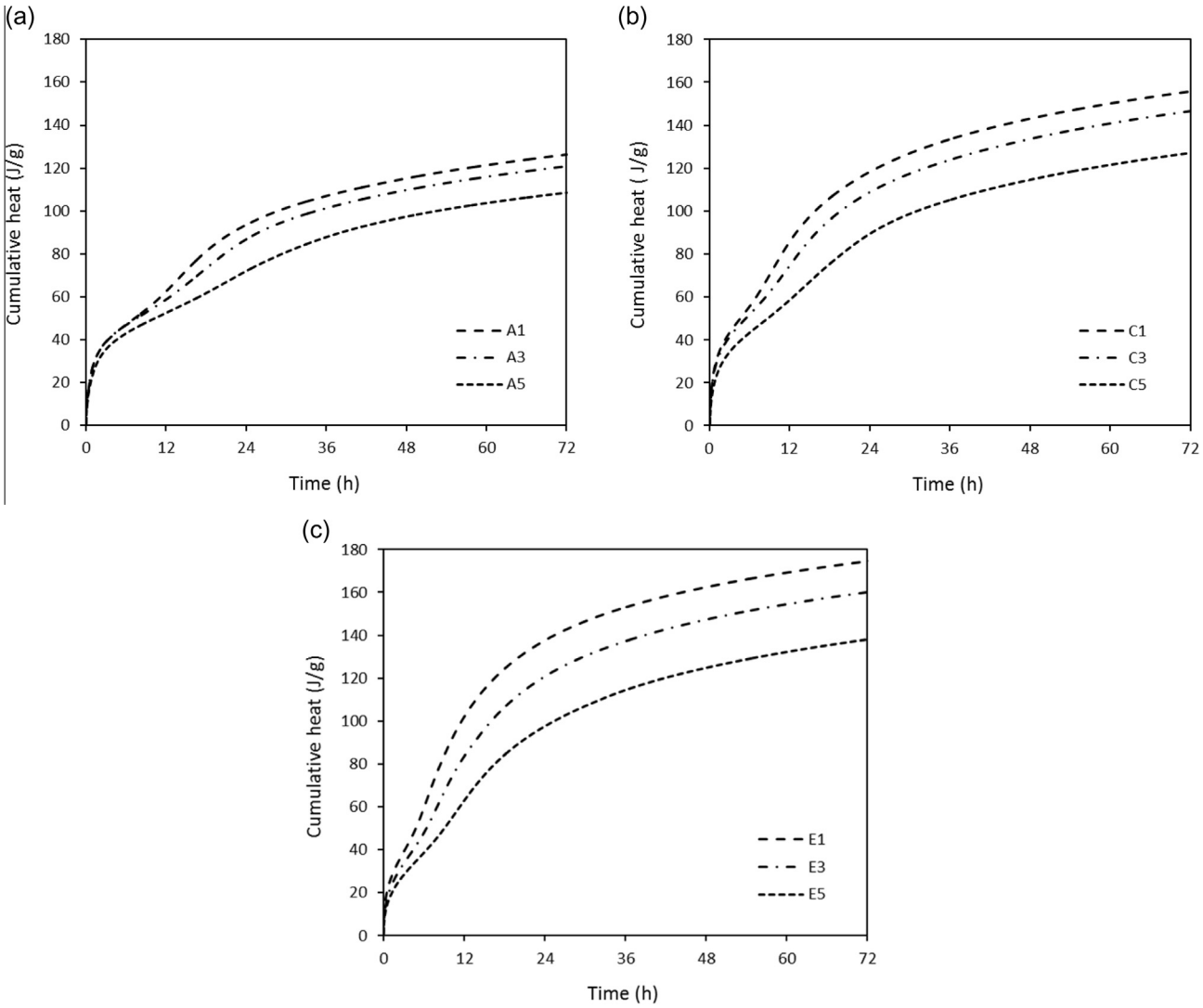

Fig. 2. Cumulative heat evolution of AA-slag/fly ash blends [with activator moduli of 1.8 (a), 1.4 (b) and 1.0 (c)].

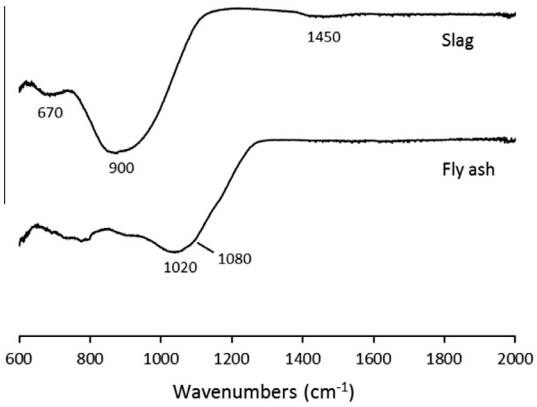

Fig. 3. FTIR spectra of solid raw materials.

matic increase between 6 to 24 h. It can be seen that for a constant activator modulus, samples with a higher slag content exhibit higher total heat release, indicating that slag presents a higher reactivity than fly ash under ambient temperature; while for a constant slag/fly ash mass ratio, higher cumulative heat evolution appears in samples with lower activator modulus, this is owing to the better reactivity of both slag and fly ash in high alkalinity conditions. The activator modulus has a more significant influence on the duration of induction time than slag/fly ash mass ratio, but both activator modulus and slag/fly ash mass ratio show a significant influence on the total heat release of acceleration/deceleration period. Additionally, it should be noted that the heat release after 24 h consists of about 20% to 35% of the total heat release within the first 72 h, this value increases with the increase in fly ash content and activator modulus, which demonstrates that the reaction process at longer ages still plays an important role in total reaction degree, especially for the samples with relatively low reactivity at early stages.

3.2. Fourier Transform infrared spectroscopy (FTIR)

The influence of activator modulus and slag/fly ash mass ratio on gel character was investigated by FTIR. Fig. 3 shows the infrared spectra of the unreacted slag and fly ash. The main vibration band for slag is at around 900 cm^{-1} and about 1020 cm^{-1} for fly ash, which is associated with the asymmetric stretching vibration of Si—O—T bonds (where T represents tetrahedral Si or Al units) [52]. The difference in the main band wavenumber is attributed to the different glassy phase structure of raw materials. The unreacted slag also shows an absorption band at around 670 cm^{-1}, which is associated with the asymmetric stretching vibration of tetrahedra T—O groups [53]. A small band at around 1450 cm^{-1} is also observed in slag, this band is corresponding to the asymmetric stretching vibration of O—C—O bonds [54], which may indicate that a slight degree of carbonation has already taken place in the raw material. For the fly ash, absorption bands located at around 1080, and 600 to 800 cm^{-1} indicate the presence of small amount of quartz [55].

Fig. 4 shows the infrared spectra of samples with the activator moduli of 1.8, 1.4, 1.0 (represented by A, C, E) and slag/fly ash mass ratios of 90/10, 70/30, 50/50 (represented as 1, 3, 5 respectively) after alkali activation. It can be seen that, regardless of the activator modulus and raw materials' relative content, all specimens exhibit similar location of absorption bands in general. Specifically, all samples showed OH groups at 1640 cm^{-1} and around 3200 cm^{-1} (since this is the only significant absorption bands after 2000 cm^{-1}, wavenumbers from 2000 to 4000 cm^{-1} are not shown in this figure), which indicates the presence of chemically bound water within the hydration products [56]. The absorption bands at around 1420 cm^{-1} in all mixes correspond to the stretching vibrations of O—C—O in carbonates [42], and this band is more significant than that in the raw material, which reveals that the occurrence of carbonation during the reaction or curing process. It should be noted that for a constant activator modulus, there is no significant change in the intensity and shape of carbonate absorption bands when changing the slag/fly ash mass ratio, but when shifting the activator modulus with a constant slag/fly ash mass ratio, slight changes take place. For instance, when comparing the samples with activator modulus of 1.8 (mix A) and 1.4 (mix C) respectively, the change in the absorption band is negligible. However, the absorption area becomes smoother and broader when the activator modulus decreases to 1.0 (mix E). It may reveal that the carbonation potential in alkali activated slag/fly ash blends has a more direct relation with activator modulus than the composition of solid raw materials. Considering that the FTIR spectra provides limited information about the quantitative analysis, more

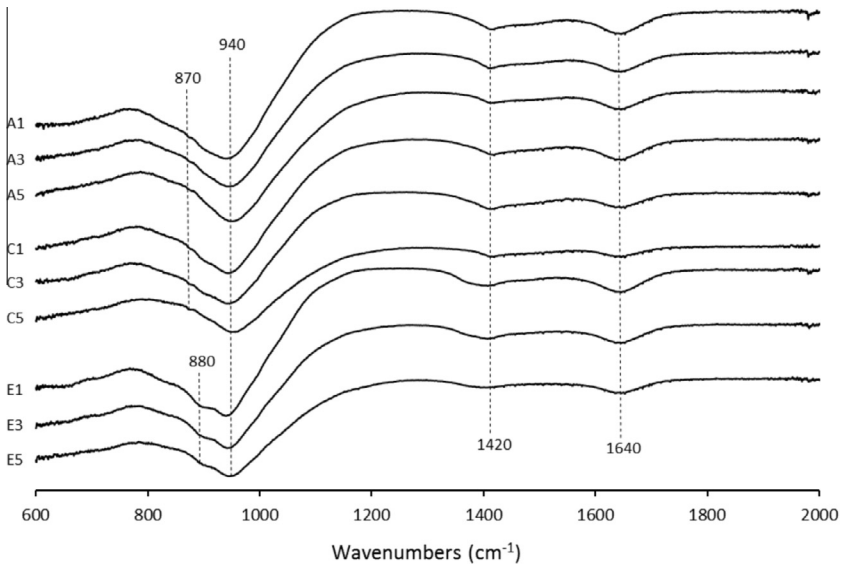

Fig. 4. FTIR spectra of alkali-activated slag/fly ash blends.

studies are needed to be carried out in order to identify the carbonation behavior of slag/fly ash blends in detail.

The main absorption band at 940 cm^{-1} is assigned to the asymmetric stretching vibration of Si—O terminal bonds [57], also represented as non-bridging structures such as Si—O—Na [58]. This is the representative vibration bands of alkali activated slag that indicate the formation of C-A-S-H type gels with short chain structures. This Si—O bond was originally located at around 900 cm^{-1} in the unreacted slag; an increase in wavenumber indicates a higher polymerized Si—O network. The vibration of main Si—O—T bonds in this study shows a lower wavenumber than previous researches [24,42,52,56], this is probably due to the nature of the slag used in this study. It can be seen that when changing the slag/fly ash mass ratio or activator modulus, the main Si—O—T vibration bonds remain stable at 940 cm^{-1} in all mixes. It is generally concluded that the shifting of the absorption wavenumbers represents the changes of polymerization degree of a certain group, thus the unchanged main absorption band indicates that both fly ash incorporation and the amount of extra silicate from activator have limited influence on the polymerization degree of hydrated gels in slag dominated alkali activated slag/fly ash blends. This is consistent with the previous study that a low fly ash inclusion has limited effect on the gel networks of slag/fly ash mixtures [24]. Under ambient temperature and high slag content conditions, due to the low reactivity of fly ash and high dissolution rate of slag, the massive presence of Ca^{2+} in the solution prefers the formation of C-A-S-H type gels. The polymerization degree of C-A-S-H gel seems to be limited by its chain structure, thus there are no significant shifts in the absorption wavenumbers when changing the slag/fly ash mass ratio and activator modulus.

It can be noted that the absorption bands around 1000 to 1100 cm^{-1}, which are usually identified from alkali activated fly ash, are not observed in all mixtures. The absorption bands around this wavenumber are assigned to the asymmetric stretching vibration of Si—O—T bridge bonds [59], which usually represent the high crosslinking networks such as silicate and alumina dominated geopolymers structures. The absence of this absorption band indicates that the typical structure of N-A-S-H gels is not formed within the reaction products. One possible explanation is that the formation of N-A-S-H type gels requires the presence of soluble silica and alumina monomers in the solution, when those monomers reach a high concentration, the formation of oligomers and the following polymerization take place. Also, the alkali cations participate in the reaction process as a charge balancer of tetrahedra T—O units. However, due to the vulnerable calcium enriched glassy structure of slag, large amounts of calcium are present in the solution at early ages, the silica and alumina units in the solution prefer to react with calcium to form precipitable C-A-S-H gels rather than continuously accumulating. The formation of C-A-S-H type gels reduces the concentration of Si, Al groups and consumes the alkali cations that are necessary for geopolymerization. Because of the calcium content is dominating in the mixes and the fly ash exhibits a low reactivity under ambient temperature, there may have no extra Si and Al existing after the calcium is fully consumed, or the remaining concentrations of Si, Al and alkalis are not sufficient enough to promote the formation of high polymerized structure.

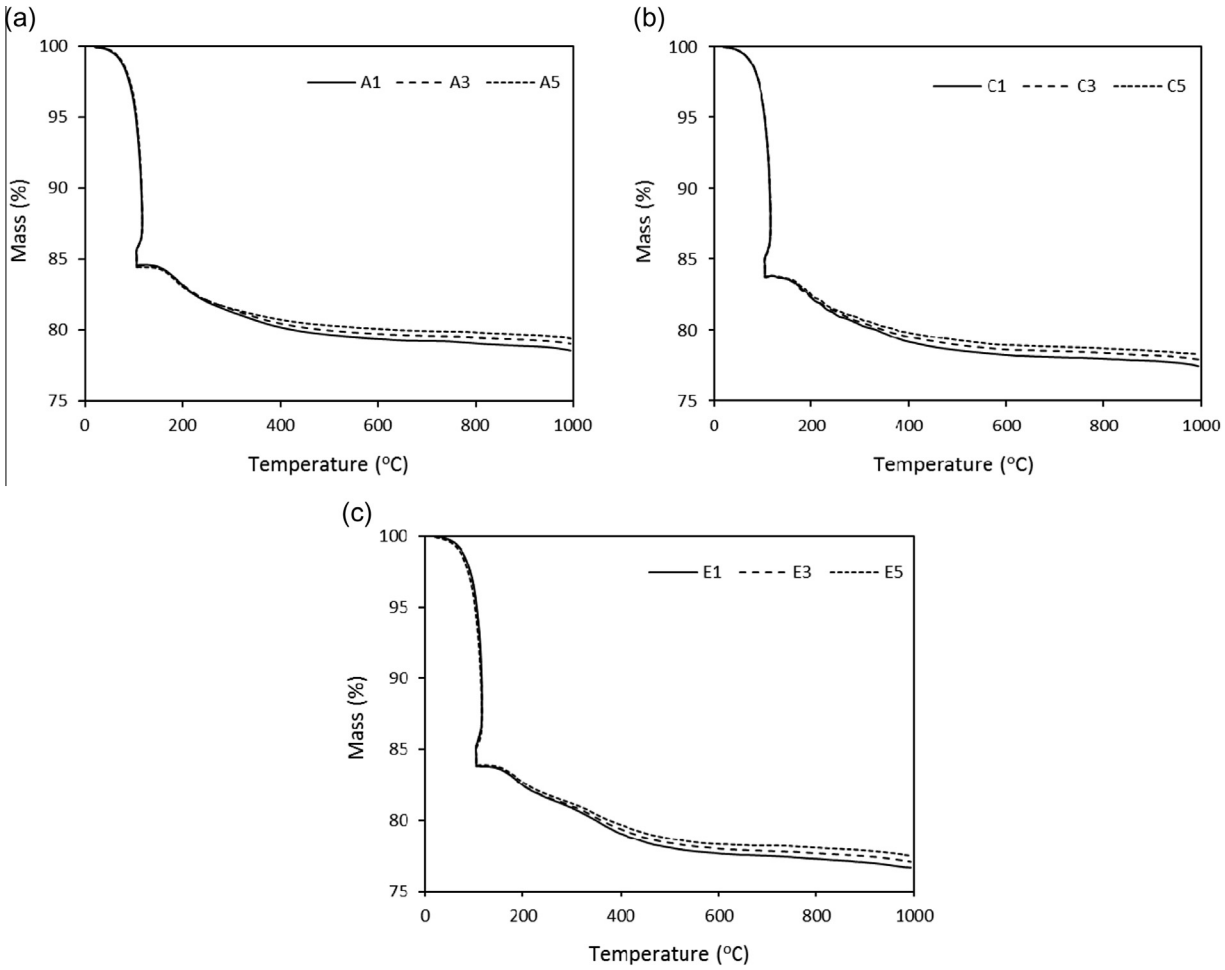

Fig. 5. TG analysis of AA-slag/fly ash blends [with activator moduli of 1.8 (a), 1.4 (b) and 1.0 (c)].

The absorption band at around 870 cm^{-1} that is associated with vibrations of Si—O terminal structures is observed in samples with activator modulus of 1.8 and 1.4 (mix A and C), and it is independent of slag/fly ash mass ratios, showing again that the reaction products are a short range C-A-S-H enriched type gels [60]. When decreasing the activator modulus to 1.0 (mix E), this absorption band disappears and a new band at around 880 cm^{-1} that represents the Si—OH bending vibration appears [61,62], this is probably due to the reduced extra silica from activator and increased alkalinity caused by the decreased activator modulus. Thus lowering the activator modulus to a certain level will lead to the structural changes to some degree.

3.3. Thermogravimetry/differential scanning calorimetry (TG/DSC)

The thermogravimetry results of all specimens are presented in Fig. 5. It can be seen that all samples exhibit a significant mass loss before around 110 °C, this is mainly due to the loss of physically bound water within the matrix [63]. The evaporable water content is around 15.5% in samples with an activator modulus of 1.8 (mix A), a slightly higher content of approximately 16.2% is observed in mixes with lower activator moduli (1.4 of mix C and 1.0 of mix E). The physically bound water content in the reaction products seems to be independent of the slag/fly ash mass ratio; also the activator modulus shows a very limited influence. After a negligible mass loss between 105 and 180 °C all samples show a gradual decrease in mass until heated to around 600 °C, followed by a stable curve with remarkably low mass loss between 600 and 1000 °C. The mass loss after 180 °C is attributed to the gradual decomposition of reaction products (mainly C-A-S-H type gels). For a constant activator modulus, samples with a higher slag content show a higher total mass loss up to 1000 °C; while for a constant slag/fly ash mass ratio, samples with a lower activator modulus present a higher total mass loss. The mass losses after 105 °C in mixes with an activator modulus of 1.8 are from 6.05% to 5.02% when changing the slag content from 90% to 50%, this value is 6.27% to 5.5% in mix C and 7.2% to 6.39% in mix E, indicating that there is a very slight but distinguishable difference in thermal properties when changing the activator modulus or slag/fly ash mass ratio. It should be noted that there are no other abrupt mass losses observed between 105 and 1000 °C, which reveals that the reaction products of alkali activated slag/fly ash blends are mainly amorphous gels with the physically and chemically bound water.

Fig. 6 shows the differential scanning calorimetry (DSC) results of all samples. The first sharp heat absorption peak at 110 °C is associated with the evaporation of physically bound water, as substantial mass loss observed at the same temperature range in the TG analysis. A smooth and broad peak with significantly low intensity appears at around 180 °C in all samples, the location of this peak corresponds to the beginning of the gradual mass loss after 105 °C in TG results, indicating the initial decomposition of the main hydrated products. Previous research on the high temperature behavior of alkali activated slag also showed that the structural deterioration of C-A-S-H type gels begins at around 200 °C [52]. Over 180 °C, the gradual decomposition processes of hydrated gels containing the loss of chemical bond water and the following gel structure changes take place. It should be noted that the temperature of initial gel deterioration remain constant regardless of

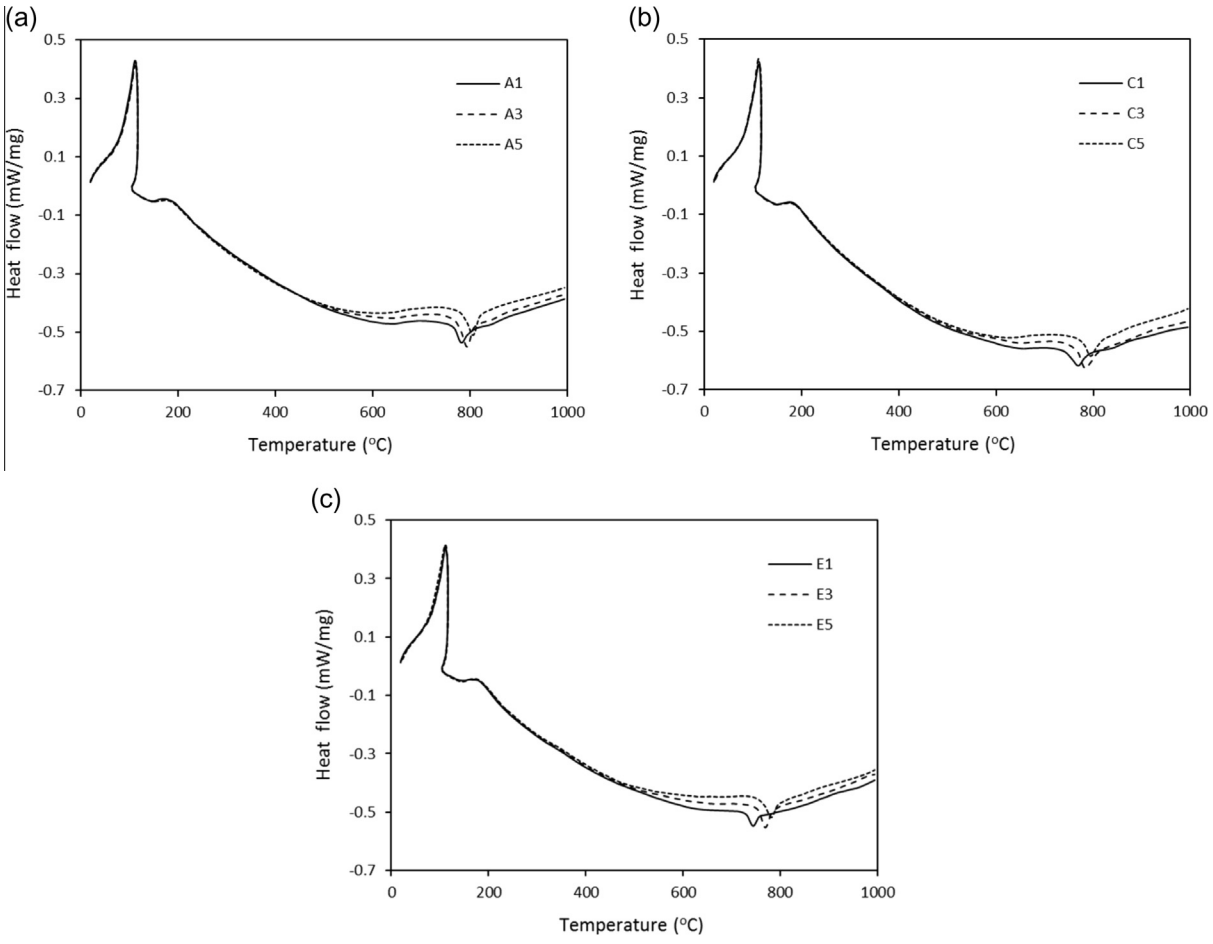

Fig. 6. DSC analysis of AA-slag/fly ash blends [with activator moduli of 1.8 (a), 1.4 (b) and 1.0 (c)].

the changes in activator modulus and slag/fly ash mass ratio, also similar TG/DSC curves before 800 °C are shown in all mixtures, revealing that the reaction products of slag dominated alkali activated slag/fly ash blends present similar thermal characteristics in general within this temperature range, even though the raw material composition is significantly changed.

All samples show an exothermic peak in the DSC curves at around 800 °C, while no remarkable changes appear in mass loss at the same temperature. The heat release at about 740 to 810 °C is due to the formation of new crystalline phases. The study of Rovnaník et al. showed that the C-A-S-H type gels completely lose the binding water when heated up to 800 °C, and the destroyed gel structure starts to form more ordered crystalline phases [52]. It can be seen that both slag/fly ash mass ratio and activator modulus are related to the location of this calorimeter peak: regardless of the activator modulus, samples with a higher slag content exhibit a lower temperature of crystallization; while under the same slag/fly ash mass ratio, a lower activator modulus presents a lower crystallization temperature. The raw material composition seems to have a more significant effect on this structural transformation.

3.4. Compressive strength

The compressive strength of samples with different starting material compositions and activator parameters after 7 days' curing is shown in Fig. 7. The collected data were having a standard deviation within 5%. It can be seen from Fig. 7 that all samples exhibit satisfying compressive strength (between 56.24 MPa and 82.18 MPa) after 7 days' curing under ambient temperature. The compressive strength decreases when increasing the fly ash content in general. For a constant activator modulus, higher compressive strengths are observed in samples with higher slag contents in all cases, but the strength difference caused by slag content becomes less significant with the decrease of the activator modulus. The activator modulus has different effects on specimens with different fly ash substitution levels: for samples with a slag/fly ash mass ratio of 90/10, the highest compressive strength of 82.2 MPa is observed with an activator modulus of 1.8, then the strength decreases continuously as the decrease of activator modulus, reaching the lowest strength of 74.2 MPa at the activator modulus of 1.0; while for samples with the slag/fly ash mass ratios of 80/20 and 70/30, the optimal activator modulus moves slightly lower to 1.6, and the compressive strength is 75.3 MPa and 72.4 MPa, respectively. Then a gradual reduction of strength takes place in both mixes, and the reduction rate is more prominent in the 70/30 mixes. On the contrary, for samples with higher fly ash contents such as 40% or 50% by mass, the compressive strength increases in general as the decrease of the activator modulus, and the highest strength appears at the Ms of 1.4 for 40/60 mixes (67.1 MPa) and 1.2 for 50/50 mixes (62.5 MPa).

The compressive strength of specimens at the ages of 28 days is given in Fig. 8. The samples showed compressive strengths ranging from 71.6 MPa to 100.9 MPa, which is promising for high performance applications. It is obvious that a higher slag content leads to a higher compressive strength in general, which is similar to the 7 days strength results. As the activator modulus decreases, the strength variations are smaller when compared to the trend in 7 days. It may indicate that the influence of raw material composition on strength becomes more significant at longer ages. When the slag/fly ash mass ratio is kept constant, all mixes show a shift in optimal activator modulus for compressive strength. It is also similar with the tendency in 7 days' results that mixes with a higher slag content have a higher optimal activator modulus, and a lower slag content exhibits a lower critical modulus. It should be noted that there is an obvious increase in the compressive strength when the activator modulus decreased from 1.8 to 1.6 or increased from 1.0 to 1.2, which is different from 7 days results. It reveals that either a high or low modulus may have negative influence on strength at longer ages. The compressive strength is increased by 25% to 30% for most of the specimens between 7 and 28 days and the increasing rates have weak correlations with either slag/fly mass ratio or activator modulus.

It can be concluded from Figs. 7 and 8 that both slag/fly ash mass ratios and activator modulus have significant influence on compressive strength. The glassy phases of slag is more vulnerable to alkaline attack than the aluminosilicates enriched ones from fly ash under room temperature [24,64], and the slag generally has a higher content of reactive phase than fly ash [65,66], thus a higher amount of Si and Ca will dissolve and more hydrated gels will be formed than fly ash, which can explain the decrease in compressive strength at both 7 and 28 days when the fly ash content is increased. It can be seen that samples with higher slag/fly ash mass ratios show a higher optimal activator modulus for strength, and this trend is more significant at early ages. This phenomenon is in accordance with the previous conclusions that a relatively high activator modulus has a positive effect on the dissolution of calcium and the formation of C-(A)-S-H gels [67], while a lower modulus has an opposite influence on the solubility of calcium from

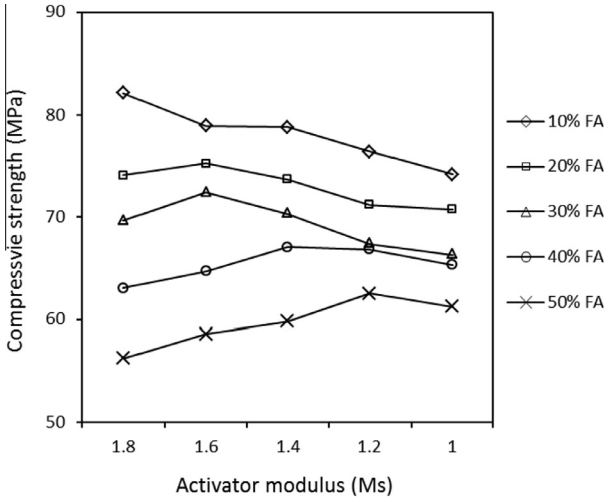

Fig. 7. Compressive strength of alkali activated slag/fly ash blends at 7 days.

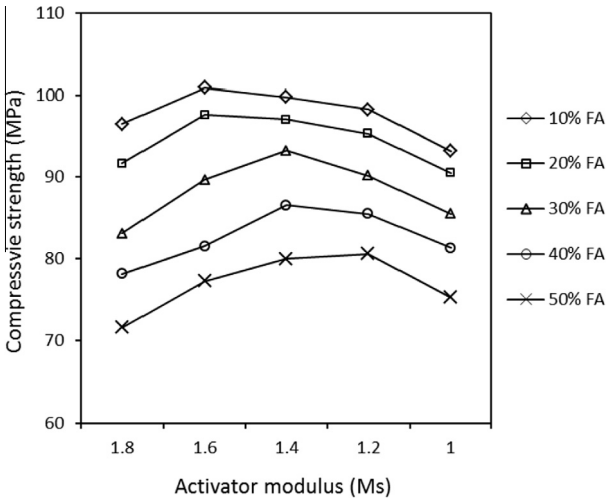

Fig. 8. Compressive strength of alkali activated slag/fly ash blends at 28 days.

Table 3
Summary of the influences of activator modulus and slag/fly ash mass ratio on the reaction and gel structure characters.

Analysis	Concerns	Activator modulus: from 1.8 to 1.4 and 1.0	Slag/fly ash ratio: from 5/5 to 7/3 and 9/1
Isothermal calorimeter	Acceleration peak intensity	Increased 64.6%, 158.6%	Increased 47.0%, 88.8%
	Acceleration peak location	Decreased 34.1%, 53.9%	Decreased 23.4%, 39.3%
	Total heat evolution	Increased 21.0%, 32.9%	Increased 14.5%, 21.9%
FTIR	Main absorption bands	Unchanged	Unchanged
	Terminal Si—O bands	Shift to 880 cm^{-1} in Ms of 1.0	Unchanged at 870 cm^{-1}
TG/DSC	Physically bond water content	Negligible change	Unchanged
	Gel decomposition temperature	Unchanged	Unchanged
	Total mass loss until 1000 °C	Slightly increased	Slightly increased
	Crystallization temperature	Decreased	Decreased

slag [19,38]. As the fly ash content increases to a certain level, a relatively low activator modulus benefits the reaction process of Si and Al dominated structures of fly ash and leads to an increase in strength [68]. Another possible explanation is that since the total Na_2O content is kept constant for all samples, a higher activator modulus provides a higher amount of extra silicate, mixes with different slag/fly ash mass ratios may exhibit different extra silicate demand to form an ideal gel structure, and the slag seems to exhibit a higher demand than fly ash under ambient temperature. The shifts in the optimum compressive strength indicate that the activator modulus and slag/fly ash ratio possess a synergetic influence on strength, thus in order to achieve a desired strength, it is suggested to determine these two parameters simultaneously.

3.5. The synergetic effects of activator and solid precursors

The starting materials of silicate activated slag/fly ash blends consist of liquid activator (sodium silicate and sodium hydroxide), solid precursors (slag and fly ash) and water. When the total Na_2O content, water/binder ratio and curing temperature are kept constant, the activator modulus and raw materials' relative content turn to be the only two dominating factors that influence the properties. These two compositional factors exhibit synergetic influences on a series of characters including the reaction kinetics, gel characters and compressive strength under ambient temperature. Table 3 summarizes the influences of raw material, activator changes on early age reaction and gel structures. As concluded in Section 3.1, the early age reaction processes can be significantly accelerated by reducing the activator modulus and increasing the slag/fly ash mass ratio. It can be seen from Table 3 that within the compositional ranges in this paper, the activator modulus exhibits a higher average increasing rate, indicating that the activator modulus shows a more significant influence on the early age reaction. This is because increasing the slag/fly ash mass ratios accelerates the reaction by increasing the total amount of high reactive phase, while lowering the activator modulus will show a more direct influence by remarkably increasing the alkalinity and providing extra silicate supply in a liquid form. Even though great changes take place in the early reaction stage, the main features of hydrated gel remain unchanged such as main Si—O—T structures, physically bound water content and thermal behaviors. It manifests that the main reaction products of alkali activated slag/fly ash blends in room temperature perform relatively stable properties regardless of the raw material composition and early reaction processes. But slight changes in terminal Si—O bonds and total mass loss show that the two investigated factors could cause the structural changes to some extent, and the gel characters may change in a more significant way if larger compositional ranges are used.

Fig. 9 shows the relationships between the total Ca/Si molar ratio and the compressive strength after 7 and 28 days of curing,

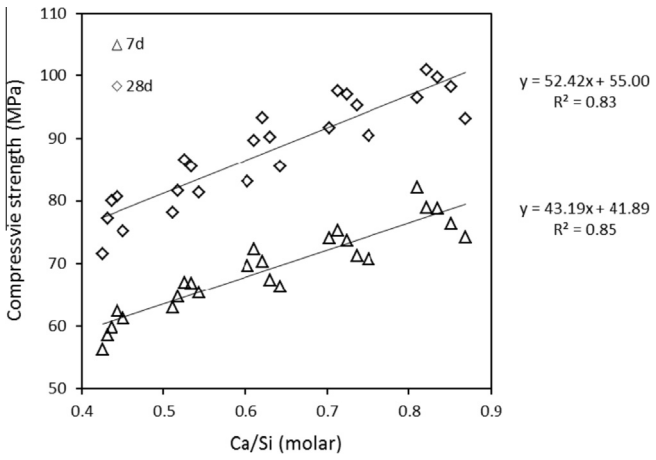

Fig. 9. The effect of Ca/Si molar ratio on the compressive strength.

where the chemical composition of the starting materials, including solid precursors and liquid activator, are computed into the molar content. There are five obviously divided groups in both curing ages, this is due to the differences in slag/fly ash mass ratio, while the five points scattered in each group is caused by the changes in activator modulus. This figure shows clearly that although slag/fly ash mass ratio has a dominating influence on the total Ca/Si ratio, the activator modulus still has a non-ignorable effect. Actually the extra silicate that is provided by the activator contains 6 to 9% by mass of the total binder (from activator modulus 1.0 to 1.8). It can also be found that the calcium content is positively related to the compressive strength in general, which is also confirmed by [19,69]. Considering that all samples have a calcium dominated gel structure, possible explanations for the calcium related strength results are: higher calcium content represents higher amount of reactive phases and more reaction products in the matrix; and/or C-A-S-H type gels exhibit an intrinsic higher strength than other type of gels. It should be noted that the strength variation caused by the activator modulus is comparable with the effects of slag/fly ash mass ratio to some extent, and samples with a lower calcium content could still show a higher strength by adjusting the activator modulus. It reveals that silicate content is as important as calcium content in terms of compressive strength. Thus determining these two factors simultaneously in the mix design stage is of great importance.

4. Conclusions

This paper investigates the synergetic effects of activator modulus and slag/fly ash mass ratios on reaction kinetics, hydrated gel

structures and compressive strength of room temperature cured alkali activated slag–fly ash blends. The activator modulus ranges from 1.0 to 1.8 and slag/fly ash mass ratios are between 90/10 to 50/50. The following conclusions can be drawn:

- All samples show the same typical reaction stages including initial dissolution, induction, acceleration, deceleration and stable period. The initial dissolution time is independent of slag/fly ash mass ratio and activator modulus, but the dissolution and reaction intensity, induction time, are strongly influenced by these two factors. Both increasing the slag/fly ash ratio and lowering the activator modulus would significantly increase the reaction intensity and shorten the main reaction processes, and activator modulus has a more significant influence than slag/fly ash ratio.
- The major reaction products in all mixes are C-A-S-H type gels with chain structure, the formation of this gel is attributed to the massive amount of available calcium in the solution. Highly polymerized N-A-S-H structures are not observed within the mentioned compositional range. Changing the activator modulus and slag/fly ash content within the mentioned range shows very limited influence on the main gel structure. But when lowering the activator modulus to 1.0, FTIR shows the absence of Si—O terminal bonds at 870 cm^{-1} and the appearance of Si—OH bonds at 880 cm^{-1}.
- All samples show similar thermal properties such as the physically bound water content and gel decomposition temperature, and these characters are independent of activator modulus and slag/fly ash mass ratio. But lowering the activator modulus and increasing the slag/fly ash ratio will slightly increase the total mass loss and decrease the phase changing temperature.
- The compressive strength results show that when increasing the slag/fly ash mass ratios, the optimum activator modulus shifts to higher values in general, this tendency is more significant in early ages. But either too high or too low modulus (1.8 or 1.0 in this case) will lead to relatively low strength. The changes in the optimum parameters in strength indicate that both slag/fly ash ratio and activator modulus are dominating factors, and in order to achieve a desired strength, these two parameters should be considered simultaneously.

Acknowledgements

This research was supported by China Scholarship Council (China) and the Department of the Built Environment, Eindhoven University of Technology (the Netherlands). The authors gratefully thank Mr. P. de Vries (ENCI B.V., the Netherlands) and Mr. J. van Eijk (Knauf Insulation), the Netherlands) for the materials supply. Furthermore, the authors wish to express their gratitude to the following sponsors of the Building Materials research group at TU Eindhoven: Rijkswaterstaat Grote Projecten en Onderhoud; Graniet-Import Benelux; Kijlstra Betonmortel; Struyk Verwo; Attero; Enci; Provincie Overijssel; Rijkswaterstaat Zee en Delta-District Noord; Van Gansewinkel Minerals; BTE; V.d. Bosch Beton; Selor; Twee "R" Recycling; GMB; Schenk Concrete Consultancy; Geochem Research; Icopal; BN International; Eltomation; Knauf Gips; Hess AAC Systems; Kronos; Joma; CRH Europe Sustainable Concrete Centre; Cement & Beton Centrum; Heros and Inashco (in chronological order of joining).

References

[1] Fernández-Jiménez A, Palomo JG, Puertas F. Alkali-activated slag mortars: mechanical strength behavior. Cem Concr Res 1999;29:1313–21.
[2] Wang SD, Scrivener KL, Pratt PL. Factors affecting the strength of alkali-activated slag. Cem Concr Res 1994;24(6):1033–43.
[3] Criado M, Fernández-Jiménez A, De la Torre AG, Aranda MAG, Palomo A. An XRD study of the effect of the SiO_2/Na_2O ratio on the alkali activation of fly ash. Cem Concr Res 2007;37:671–9.
[4] Bakharev T. Durability of geopolymer materials in sodium and magnesium sulfate solutions. Cem Concr Res 2005;35:1233–46.
[5] Bakharev T, Sanjayan JG, Cheng YB. Resistance of alkali-activated slag concrete to acid attack. Cem Concr Res 2003;33:1607–11.
[6] Fernández-Jiménez A, García-Lodeiro I, Palomo A. Durable characteristics of alkali activated fly ashes. J Mater Sci 2007;42:3055–65.
[7] Fernández-Jiménez A, Palomo A, López-Hombrados C. Some engineering properties of alkali activated fly ash concrete. ACI Mater J 2006;103:106–12.
[8] Kong DLY, Sanjayan JG. Damage behavior of geopolymer composites exposed to elevated temperatures. Cem Concr Compos 2008;30:986–91.
[9] Hai YZ, Venkatesh Kodur, Shu LQ, Liang C, Bo W. Development of metakaolin-fly ash based geopolymers for fire resistance applications. Constr Build Mater 2014;55:38–45.
[10] Weil M, Dombrowski K, Buchawald A. Life-cycle analysis of geopolymers. Geopolymers, structure, processing, properties and applications. Abington Hall: Woodhead Publishing Limited; 2009. p. 194–210.
[11] Chao Li, Henghu Sun, Longtu Li. A review: the comparison between alkali-activated slag (Si + Ca) and metakaolin (Si + Al) cements. Cem Concr Res 2010;40:1341–9.
[12] Brough AR, Atkinson A. Sodium silicate-based alkali-activated slag mortars: Part I. Strength, hydration and microstructure. Cem Concr Res 2002;32:865–79.
[13] Granizo ML, Alonso S, Blanco-Varela MT, Palomo A. Alkaline activation of metakaolin: effect of calcium hydroxide in the products of reaction. J Am Ceram Soc 2002;85(1):225–31.
[14] Lee NK, Lee HK. Setting and mechanical properties of alkali-activated fly ash/slag concrete manufactured at room temperature. Constr Build Mater 2013;47:1201–9.
[15] Rashad Alaa M. Properties of alkali-activated fly ash concrete blended with slag. Iran J Mater Sci Eng 2013;10(1):57–64.
[16] Aydin S. A ternary optimization of mineral additives of alkali activated cement mortars. Constr Build Mater 2013;43:131–8.
[17] Sugama T, Brothers LE, Van de Putte TR. Acid-resistant cements for geothermal wells: sodium silicate activated slag/fly ash blends. Adv Cem Res 2005;17(2):65–75.
[18] Escalante García JI, Campos-Venegas K, Gorokhovsky A, Fernández A. Cementitious composites of pulverised fuel ash and blast furnace slag activated by sodium silicate: effect of Na_2O concentration and modulus. Adv Appl Ceram 2006;105(4):201–8.
[19] Yip CK, Lukey GC, van Deventer JSJ. The coexistence of geopolymeric gel and calcium silicate hydrate at the early stage of alkaline activation. Cem Concr Res 2005;35:1688–97.
[20] García-Lodeiro I, Fernández-Jiménez A, Palomo A, Macphee DE. Effect of calcium additions on N-A-S-H cementitious gels. J Am Ceram Soc 2010:1–7.
[21] García-Lodeiro I, Macphee DE, Palomo A, Fernández-Jiménez A. Effect on fresh C-S-H gels the simultaneous addition of alkali and aluminium. Cem Concr Res 2010;40:27–32.
[22] García-Lodeiro I, Fernández-Jiménez A, Blanco MT, Palomo A. FTIR study of the sol-gel synthesis of cementitious gels: C-S-H and N-A-S-H. J Sol-Gel Sci Techn 2008;45:63–72.
[23] García-Lodeiro I, Macphee DE, Palomo A, Fernández-Jiménez A. Effect of alkalis on fresh C-S-H gels. FTIR analysis. Cem Concr Res 2009;39:147–53.
[24] Ismail I, Bernal SA, Provis JL, Nicolas RS, Hamdan S, Deventer JSJ. Modification of phase evolution in alkali-activated blast furnace slag by the incorporation of fly ash. Cem Concr Compos 2014;45:125–35.
[25] Duxson P, Provis JL, Lukey GC, Mallicoat SW, Kriven WM, Deventer JSJ. Understanding the relationship between geopolymer composition, microstructure and mechanical properties. Colloids Surf A 2005;269:47–58.
[26] Caijun Shi, Fernández Jiménez A, Palomo A. New cements for the 21st century: the pursuit of an alternative to Portland cement. Cem Concr Res 2011;41:750–63.
[27] Shen WG, Wang YH, Zhang T, Zhou MK, Li JS, Cui XY. Magnesia modification of alkali-activated slag fly ash cement. J Wuhan Univ Technol Mater Sci Ed 2011;26:121–5.
[28] Kumar S, Kumar R, Mehrotra SP. Influence of granulated blast furnace slag on the reaction, structure and properties of fly ash based geopolymer. J Mater Sci 2010;45(3):607–15.
[29] Chi M, Huang R. Binding mechanism and properties of alkali-activated fly ash/slag mortars. Constr Build Mater 2013;40:291–8.
[30] Yang T, Yao X, Zhang ZH, Wang H. Mechanical property and structure of alkali-activated fly ash and slag blends. J Sustain Cem Based Mater 2012;1:167–78.
[31] Zhang DJ, Liu WS, Hou HB, He XH. Strength, leach ability and microstructure characterization of Na_2SiO_3-activated ground granulated blast-furnace slag solidified MSWI fly ash. Waste Manage Res 2007;25:402–7.
[32] Puertas F, Martínez-Ramírez S, Alonso S, Vázquez E. Alkali-activated fly ash/slag cement. Strength behaviour and hydration products. Cem Concr Res 2000;30:1625–32.
[33] Shi C, Day RL. Early strength development and hydration of alkali-activated blast furnace slag/fly ash blends. Adv Cem Res 1999;11(4):189–96.

[34] Douglas E, Brandstetr J. A preliminary study on the alkali activation of ground granulated blast-furnace slag. Cem Concr Res 1990;20:746–56.
[35] Guerrieri M, Sanjayan JG. Behavior of combined fly ash/slag-based geopolymers when exposed to high temperatures. Fire Mater 2010;34:163–75.
[36] ASTM C 618: Standard Specification for Coal Fly Ash and Raw or Calcined Natural Pozzolan for Use in Concrete.
[37] British Standard EN 196-1:2005. Methods of testing cement Part 1: Determination of strength.
[38] Deira E, Gebregziabiher BS, Peethamparan S. Influence of starting material on the early age hydration kinetics, microstructure and composition of binding gel in alkali activated binder systems. Cem Concr Compos 2014;48:108–17.
[39] Chithiraputhiran S, Neithalath N. Isothermal reaction kinetics and temperature dependence of alkali activation of slag, fly ash and their blends. Constr Build Mater 2013;45:233–42.
[40] Brough AR, Holloway M, Sykes J, Atkinson A. Sodium silicate-based alkali-activated slag mortars Part II. The retarding effect of additions of sodium chloride or malic acid. Cem Concr Res 2000;30:1375–9.
[41] Ravikumar D, Neithalath N. Reaction kinetics in sodium silicate powder and liquid activated slag binders evaluated using isothermal calorimetry. Therm Acta 2012;546:32–43.
[42] Bernal SA, Provis JL, Rose V, Gutierrez RM. Evolution of binder structure in sodium silicate-activated slag-metakaolin blends. Cem Concr Compos 2011;33:46–54.
[43] Shi C, Day RL. A calorimetric study of early hydration of alkali-slag cements. Cem Concr Res 1995;25:1333–46.
[44] Rajaokarivony-Andriambololona Z, Thomassin JH, Baillif P, Touray JC. Experimental hydration of two synthetic glassy blast furnace slags in water and alkaline solutions (NaOH and KOH 0.1 N) at 40 °C: structure, composition and origin of the hydrated layer. J Mater Sci 1990;25:2399–410.
[45] Rimer JD, Lobo RF, Vlachos DG. Physical basis for the formation and stability of silica nanoparticles in basic solutions of monovalent cations. Langmuir 2005;21:8960–71.
[46] Bakharev T, Sanjayan JG, Cheng YB. Alkali activation of Australian slag cements. Cem Concr Res 1999;29(1):113–20.
[47] Krizana D, Zivanovic B. Effects of dosage and modulus of water glass on early hydration of alkali–slag cements. Cem Concr Res 2002;32:1181–8.
[48] Song S, Jennings HM. Pore solution chemistry of alkali-activated ground granulated blast-furnace slag. Cem Concr Res 1999;29:159–70.
[49] Rothstein D, Thomas JJ, Christensen BJ, Jennings HM. Solubility behavior of Ca-, S-, Al-, and Si-bearing solid phases in Portland cement pore solutions as a function of hydration time. Cem Concr Res 2002;32:1663–71.
[50] Criado M, Fernández-Jiménez A, Palomo A, Sobrados I, Sanz J. Effect of the SiO_2/Na_2O ratio on the alkali activation of fly ash. Part II: ^{29}Si MAS-NMR survey. Microporous Mesoporous Mater 2008;109:525–34.
[51] Fernández-Jiménez A, Palomo A. Composition and microstructure of alkali activated fly ash binder: effect of the activator. Cem Concr Res 2005;35(10):1984–92.
[52] Rovnaník P, Bayer P, Rovnaníková P. Characterization of alkali activated slag paste after exposure to high temperatures. Constr Build Mater 2013;47:1479–87.
[53] Kovalchuk G, Fernandez-Jimenez A, Palomo A. Alkali-activated fly ash: effect of thermal curing conditions on mechanical and microstructural development – Part II. Fuel 2007;86:315–22.
[54] Yousuf M, Mollah A, Hess TR, Tsai YN, Cocke DL. An FTIR and XPS Investigations of the effects of carbonation on the solidification/stabilization of cement based systems-Portland type V with zinc. Cem Concr Res 1993;23(4):773–84.
[55] Gadsden JA. Infrared spectra of minerals and related inorganic compounds. London, England: Butterworths; 1975.
[56] Yu P, Kirkpatrick RJ, Poe B, McMillan PF, Cong X. Structure of calcium silicate hydrate (C-S-H): near-, mid-, and far-infrared spectroscopy. J Am Ceram Soc 1999;82(3):742–8.
[57] Zhang ZH, Wang H, Provis JL, Bullen F, Reid A, Zhu YC. Quantitative kinetic and structural analysis of geopolymers. Part 1. The activation of metakaolin with sodium hydroxide. Therm Acta 2012;539:23–33.
[58] Lee WKW, Deventer JSJ. Use of infrared spectroscopy to study geopolymerization of heterogeneous amorphous aluminosilicates. Langmuir 2003;19:8726–34.
[59] Hajimohammadi A, Provis JL, Deventer JSJ. Time-resolved and spatially resolved infrared spectroscopic observation of seeded nucleation controlling geopolymer gel formation. J Colloid Interface Sci 2011;357:384–92.
[60] Criado M, Fernandez-Jimenez A, Palomo A. Alkali activation of fly ash: effect of the SiO_2/Na_2O ratio Part I: FTIR study. Microporous Mesoporous Mater 2007;106:180–91.
[61] Lee WKW, Deventer JSJ. Effects of anions on the formation of aluminosilicate gel in geopolymers. Ind Eng Chem Res 2002;41:4550–8.
[62] Lancellotti I, Catauro M, Ponzoni C, Bollino F, Leonelli C. Inorganic polymers from alkali activation of metakaolin: effect of setting and curing on structure. J Solid State Chem 2013;200:341–8.
[63] Kong DLY, Sanjayan JG. Effect of elevated temperatures on geopolymer paste, mortar and concrete. Cem Concr Res 2010;40:334–9.
[64] Fan Y, Yin S, Wen Z, Zhong J. Activation of fly ash and its effects on cement properties. Cem Concr Res 1999;29:467–72.
[65] Duxson P, Fernández-Jiménez A, Provis JL, Lukey G, Palomo A, Deventer JSJ. Geopolymer technology: the current state of the art. J Mater Sci 2007;42:2917–33.
[66] Fernández-Jimenez A, De La Torre AG, Palomo A, López-Olmo G, Alonso M, Aranda M. Quantitative determination of phases in the alkali activation of fly ash. Part I. Potential ash reactivity. Fuel 2006;85:625–34.
[67] Phair JW, Deventer JSJ, Smith JD. Mechanism of polysialation in the incorporation of zirconia into fly ash-based geopolymers. Ind Eng Chem Res 2000;39:2925–34.
[68] Jaarsveld JGS. The physical and chemical characteristics of fly ash based geopolymers. PhD Thesis, The University of Melbourne, 2000.
[69] Xu H, Deventer JSJ. The geopolymerisation of alumino-silicate minerals. Int J Miner Process 2000;59:247–66.